

STUDY ON HEAT TRANSFER CHARACTERISTICS OF SINGLE-LAYER DOUBLE-ROW PULSATING HEAT PIPE

by

*Fumin Shang^{1,2}, Shilong Fan^{*1}, Qingjing Yang¹, Chaoyue Liu¹, Jianhong Liu¹*

^{*1} Changchun Institute of Technology, School of Energy and Power, China Changchun 130012, China;

² Jilin Engineering Research Center for Building Energy Supply and Indoor Environmental Control, China Changchun 130012, China;

* Fumin Shang; fslwd91@126.com

The structure and inclination angle of a pulsating heat pipe are critical factors influencing the heat transfer performance and operation mode. In this work, a single-layer double-row pulsating heat pipe is designed, and the start-up and heat transfer characteristics of pulsating heat pipe at limit angles (0°, 90°, and 180°) are experimentally investigated. Also, the operation mode and heat transfer characteristics are studied through IR imager and temperature profiles. The study highlighted that the pulsating heat pipe has excellent operation characteristics in the limit angle. When the inclination angle is 0°, the double-row structure improves the start-up performance; at 90° inclination, the pulsating heat pipe starts the fastest, and the heat transfer resistance keeps the smallest in the whole test. When the inclination angle is 180°, the pulsating heat pipe has the best thermal sensitivity but weak working fluid flow capacity during operation.

Key words: pulsating heat pipe, double-row structure, start-up mode, heat transfer performance

1. Introduction

With the rapid development of the computer industry, processors increasingly consume more energy during operation. Therefore, controlling the processor temperature is an effective way to improve processor efficiency and save energy [1, 2].

There are many kinds of technology used to control the temperature at present. The heat pipe is one of the important equipment. The thermosyphon heat pipe has been studied extensively by previous scholars. Arya et al [3]. studied the plate heat pipe with carbon nanotubes nanofluid as working fluid. The application of carbon nanotubes-water nanofluid makes the heat pipe have better heat transfer performance than water. M.M. Sarefraz et al [4, 5]. studied the heat transfer characteristics of thermosyphon heat pipe with a variety of different working fluids. It was found that the zirconia-acetone nanofluid could enhance the geyser boiling and increase the transfer coefficient by 36.3%. It is

also found that n-pentane-acetone and n-pentane-methanol binary mixtures play an important role in improving the heat transfer performance of the thermosyphon heat pipe. Although thermosyphon heat pipe has good heat transfer characteristics, its complex internal structure leads to high production costs. Pulsating heat pipe is a kind of heat pipe with reliable heat transfer performance and simple structure, which has potential development direction.

In the 1990s, Akachi [6] proposed the pulsating heat pipe (PHP), a passive heat transfer device with high heat transfer efficiency, small volume, flexible arrangement, and reliable operation, which became one of the most reliable heat dissipation equipment [7, 8].

The inclination angle and structure are the main factors impacting the heat transfer performance of PHP devices [9-12]. Changing the structure to optimize the heat transfer performance is one of the simplest and most direct means to develop the advantages of the pulsating heat pipe. For example, Aboutalebiet al. [13] designed a rotating closed-loop PHP. The thermal resistance of the rotating PHP decreases with the increase of heat input at a certain filling ratio. In a specific range of heat input, the drying may occur in the evaporation section, thus deteriorating the thermal performance. With the increase of the rotating speed, the thermal resistance decreases, thereby reducing the possibility of dry in the evaporation section. Kelly et al. [14] designed a radial PHP for the local hot spot heat dissipation capable of reducing the average temperature of hot spots by 30 °C. The PHP was engraved on an annular copper plate with a diameter of 110 mm. Each channel had a rectangular groove 1mm deep and 1 mm wide. The evaporation section was located inside the annular copper plate, and the condensation section was outside the annular copper plate. Burbanel et al. [15] manufactured a non-loop pulsating heat pipe for use in automobiles, which shows good stability during operation.

The inclination angle mainly affects the effect of gravity to change the running state of the PHP, unless the PHP has more turns [16,17]. The influence of the inclination angle on the heat transfer characteristics varies slightly at different angles, so changing the angle can effectively improve the heat transfer performance [18-21]. Rahman et al. [22] focused on the heat transfer performance of a PHP at 0°, 30°, and 45° inclination. Gravity and the thermal properties of the working fluid affect the heat transfer performance of the device significantly. Li et al. [23] investigated the heat transfer characteristics at different inclination angles using a PHP with helium as the working fluid. The influence of the inclination angle is evident in the medium filling ratio (48.8%~66.1%), and inclination angles of 60° and 90° have similar heat transfer characteristics. Ghanbarpour et al. [24] and Xue et al. [11] respectively studied the heat transfer characteristics at 0°, 30°, 60°, and 90° angles. When the inclination angle is 60°, the PHP has the best heat transfer characteristics, while at 0°, the PHP is the easiest to start. Jian et al. [25] studied the flow state of the fluid when the inclination angle varied from 0° to 90° through visualization. From 60° to 90° inclination angles, the working fluid flow mode is mainly large-amplitude oscillation, and the phenomenon of dry combustion is easy to occur. Karthikeyan et al. [26] used IR camera to study the relationship between the temperature change of the wall and the working fluid flow when the inclination angle was 0°. The flow state of the working fluid directly determines the heat transfer performance of the pulsating heat pipe.

Through the above investigation, the PHP is affected by the structure and inclination angle. However, the PHP has failed to start-up and has poor heat transfer performance at limit angles (0°, 90°, and 180°). This work investigates the heat transfer performance and operation mode of a double-row PHP with communicating pipes. The method of to improve the failure of pulsating heat pipe at the limit angle and reduced heat transfer performance was found by the single-layer double-row structure.

2. Experimental setup and procedure

2.1. Experimental setup

Figure 1 shows the experimental system, which consists of a heating system, a data acquisition system, and a PHP. The heating system consists of transformers, an ammeter, and a power meter. The applied heating power was controlled by adjusting the transformer. In the evaporator section, two heating panels with each power of 1200 W were used. Insulation materials applied to the external surface of heating panels reduced heat losses. The condenser section released heat into the environment by natural convection. Figure 2 shows the layout of temperature measuring points on the evaporator section and condenser section. The measurements from 14 K-type thermocouples at T1 to T14 measuring points gave the temperature variation of the evaporator section and condenser section, and the IR camera recorded the heat flux distribution.

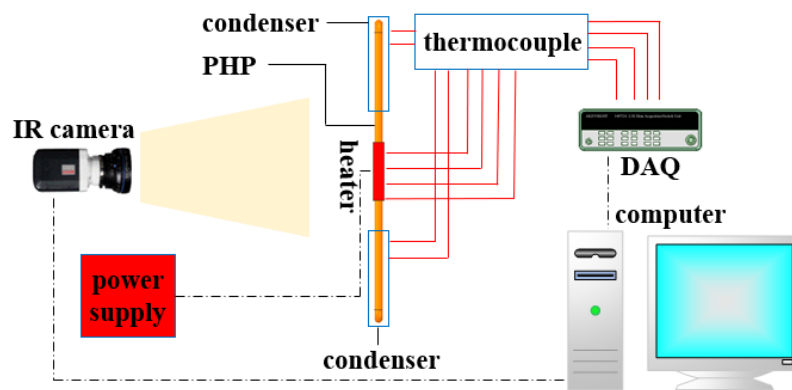


Fig. 1. Schematic of the experimental setup

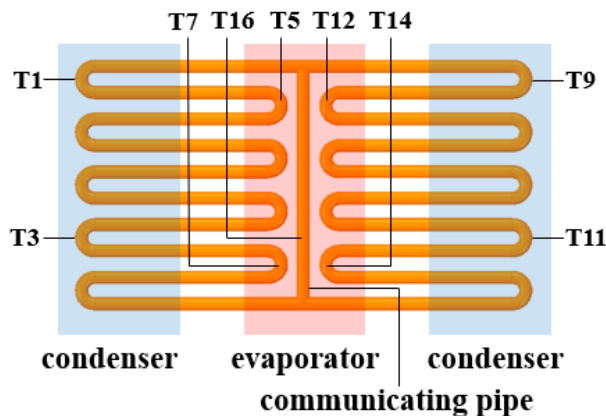


Fig. 2. Temperature measuring points

The PHP was made of ten copper U-shaped tubes with ribbed plates; each row had five channels. The length of the copper pipe in each channel was 330 mm with an inner diameter of 3 mm and an outer diameter of 5 mm. The communicating pipe length was 270 mm. The length of the evaporator section, adiabatic section, and condensers section was 80, 40, and 150 mm, respectively. The vacuum level in the system was set to 7.9 Pa. The copper pipes were filled with deionized water to a filling ratio of 50%.

The temperature of the working fluid determines the thermal and physical properties of the fluid in the copper pipe. The critical diameter of the PHP has an important relationship with the thermal and physical properties of the working fluid [27]. The critical diameter is given by:

$$d \leq d_{cr} = 2 \sqrt{\frac{\sigma}{(\rho_l - \rho_v) g}} \quad (1)$$

Where σ is the surface tension of deionized water, g is gravitational acceleration, and ρ is the density of working fluid. The diameter of the copper pipe is smaller than the critical diameter when the PHP is not heated. The surface tension of the liquid in the copper pipe plays an essential role in the distribution of the liquid column and bubbles.

2.2. Experimental procedure

Before experimenting, the seal and reliability of the PHP was tested. Under the minimum heat load, the start-up characteristics of the PHP could be demonstrated. Also, leakage problems could be avoided by not exceeding the maximum heat input.

In the experiment, the heat transfer characteristics of the PHP were first measured. In the beginning, the data acquisition system and IR imager were initialized. The power supply system was turned on to heat the PHP at the desired heat input. The IR imager recorded the temperature distribution of the PHP. Each test was carried out for 40 minutes under a given input condition to ensure the stable operation of PHP. After completing the heat input measurement, the heat power was increased by 20 W to the next condition. The procedure was repeated until the heat input reached the desired maximum of 180 W. The PHP was placed in the air and cooled to room temperature. To avoid possible influence caused by the previous angle experiment, the PHP was randomly shaken to cause the vapor plug and liquid column in the pipe to be randomly distributed before the next experiment. Figure 3 shows three angles of the experimental process, respectively.

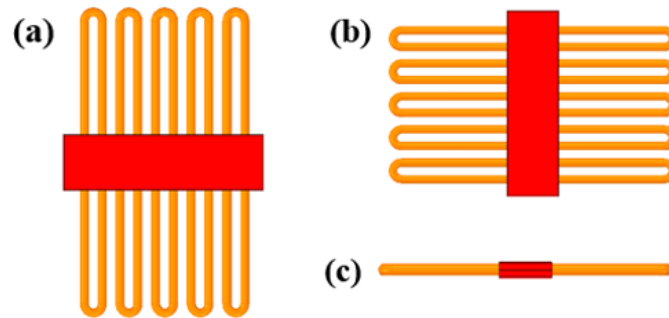


Fig. 3. Experimental inclination angles; (a) 0°; (b) 90°; (c)180°

Table 1 summarizes the maximum uncertainties of the main parameters of this study. The uncertainties of direct measurement parameters such as T_e and T_c were calculated from the system uncertainty e_s from the precision of each instrument and the random uncertainty e_r from the repeatability of data as follows:

$$e = \sqrt{e_s^2 + e_r^2} \quad (2)$$

The uncertainties of indirect measurement parameters such as Q and R were obtained by uncertainty propagation theory [28].

Table 1. Maximum uncertainties.

Parameters	\bar{T}_e	\bar{T}_c	Q	R
Uncertainty (\pm)	1.03%	2.57%	5.2%	2.7%

The experiment used the temperature profile to analyze the flow characteristics of the fluid. The operational process of the PHP can be divided into three stages, namely the start-up stage, the quasi-stable stage, and the stable stage. The temperature variation of the evaporator and condenser section of the same pipe can be used to represent the operation of the PHP. The temperature oscillation curve of the PHP was calculated based on the temperature changes of T5 and T7 measuring points.

\bar{T}_e and \bar{T}_c are average temperatures of evaporator and condenser found from the experiment, and the thermal resistance was calculated using these measured temperature values as:

$$R = \frac{\Delta\bar{T}_{e-c}}{Q} \quad (3)$$

Where $\Delta\bar{T}_{e-c}$ is the difference between \bar{T}_e and \bar{T}_c . The value of Q is the effective heat input provided to the evaporator zone [19].

3. Results and discussions

3.1. Start-up characteristics at different inclination angles

This research used a single-layer double-row channel PHP. The average temperature profile of double-row pipes is analyzed to study the heat transfer characteristics during start-up and operation stages. The start-up performance is mainly reflected in the start-up time and the start-up temperature. The start-up time and the start-up temperature reflect the rapidity and sensitivity of pulsating heat pipe, respectively. The start-up is marked by the first large peak-trough oscillation in the temperature profile after a smooth raise in the initial stage of the experiment [30]. Figure 4 (a) shows the temperature profile start-up process at 0° inclination angle. When the temperature rises smoothly, $t_A=279$ s for the temperature oscillation firstly of upper channels, and $t_B=282$ s for the temperature oscillation firstly of nether channels. Top and bottom channels start-up at different times; the start-up of top channel occurs 13 s before than that of bottom channels. An IR imager was used to deeply investigate the causes of the different start-ups of channels on both sides. Figure 4 (b) shows the capture of the IR imager at $t_B=282$ s in the start-up period. In the figure, numbers 1 to 5 are the top channels (condensing section), numbers 6 to 10 are the bottom channels (condensing section), and the white area is the heating plate (evaporation section). The temperature of the condensing section (top channels) is relatively high. With the heat accumulation, the high-temperature fluid flows from both sides of channels to middle channels, resulting in the temperature of channels 1, 2, 4, 5 are higher than that of channel 3. Channels adjacent to the lower channel shave a similar temperature distribution. From the evaporation section to the condenser section, the temperature gradually decreases. The flow capacity of the working fluid between channels is reduced. The analysis of the IR images in combination with the structure of pulsating heat pipe, high light hat top channels have more bubbles due to the influence of gravity (the filling ratio is less than 50%), and bottom channels have fewer bubbles (the filling ratio is more than 50%). In the heating process, the side with a lower filling ratio starts earlier than the side with a higher

filling ratio, so the working fluid in top channels flows first, and the working fluid in lower channels follows the start-up. This double-row arrangement overcomes the problem of starting-up when the inclination angle is 180° .

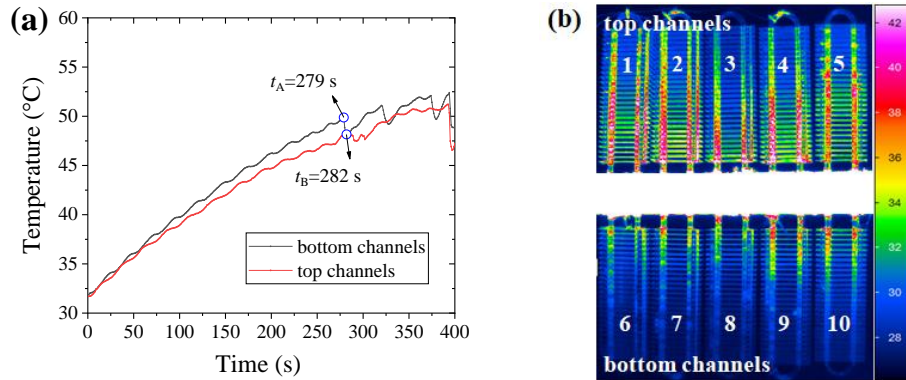


Fig. 4. The start-up performance when the inclination angle is 0° ; (a) temperature profile; (b) IR temperature profiles for start-up performance evaluation: the temperature scale is on the right.

To further study the start-up characteristics of the double-row PHP, the start-up characteristic polarity was studied when the inclination angle was 90° (i.e., the heating plate was placed vertically on the ground). Figure 5 (a) shows the temperature profile of the PHP start-up process when the inclination angle is 90° . The time for the start-up is $t_A = 209$ s, and the start-up temperature $T = 49.8$ °C. The temperature profile of both sides shows a large oscillation at the same time; namely, the working fluid of both sides flows at the same time, and both sides start synchronously. However, there is a significant difference in the flow mode of working fluid on both sides during the start-up process. Figure 5 (b) shows the IR image at $t_A = 209$ s during the start-up process. During the start-up period, the temperature difference between channels on the left side is small, while that between channels on the right side is large, and shows a decreasing trend from channel 6 to channel 10. This phenomenon indicates that poor performance of the working fluid flows for the left channels at the start-up period while that of the right channels is better.

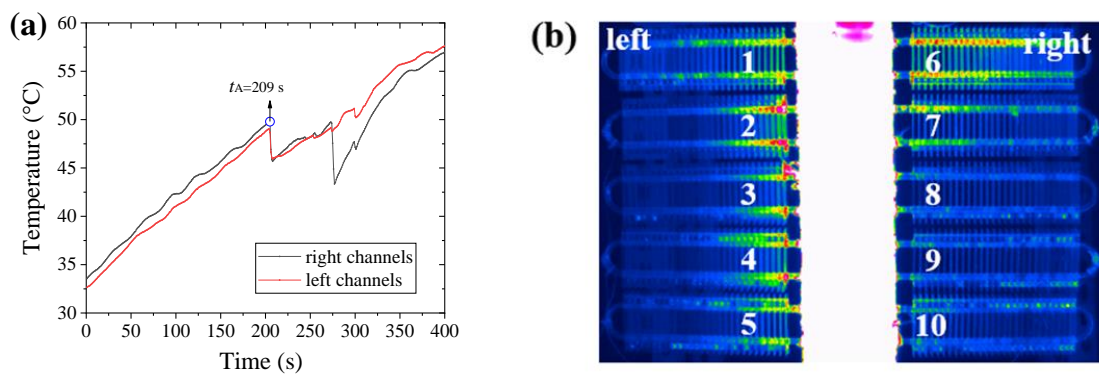


Fig. 5. The start-up performance when the inclination angle is 90° ; (a) temperature profile; (b) IR temperature profiles for start-up performance evaluation.

Figure 6 (a) shows the temperature profile during the start-up period when the inclination angle is 180° (the heating plate is parallel to the ground). The PHP has a good start-up performance with the start-up time $t_A = 248$ s and start-up temperature $T = 43.2$ °C. Figure 6 (b) shows the operation mode of the working fluid during the start-up. Left and right channels have the same temperature distribution;

the temperature gradually decreases from the evaporation section to the condensation section, and the temperature difference between adjacent channels is small. The reason for this operation mode is related to the random distribution of the gas plug and liquid plug of the working fluid in the tube when there is no external heat power input. When placed parallel to the ground, the gravity effect is negligible. The gas plug and liquid plug reach the equilibrium state; the working fluid in the tube is static. As the heat inputting, the randomly distributed working fluid absorbs the heat, which is more likely to generate pressure differential flow of working fluid. Therefore, The PHP can start-up quickly when the inclination angle is 180° .

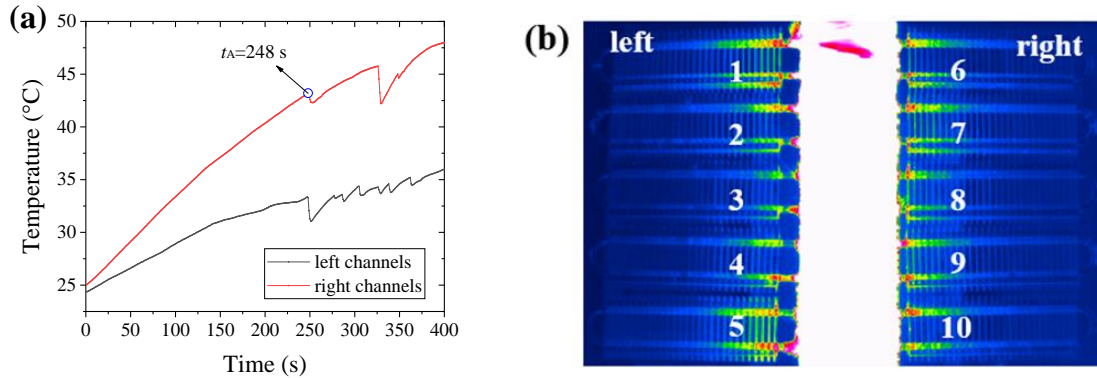


Fig. 6. The start-up performance when the inclination angle is 180° ; (a) temperature profile; (b) IR temperature profiles for start-up performance evaluation.

Table 2 shows the start-up time and temperature at different angles. Although the start-up performance is the worst for 0° inclination angle, the double-row structure improves the start-up problem when the evaporator section at the top of the PHP. At a 90° inclination angle, the start-up time is the shortest, and start-up speed is the fastest. When the inclination angle is 180° , the PHP has the lowest start-up temperature and is most sensitive to temperature.

Table 2. start-up time and temperature at different inclination angles.

angle ($^\circ$)	0	90	180
start-up time (s)	279	209	248
start-up temperature ($^\circ\text{C}$)	49.8	49.8	43.2

3.2. Operation characteristics at different inclination angles

The operation mode determines the heat transfer performance, and it has important guiding significance to study the operation characteristics under different inclination angles. Figure 7 (a) shows the temperature oscillation profile when the inclination angle is 0° . The temperature profile of upper channels has a small amplitude and high-frequency oscillation mode. The oscillation frequency of bottom channels is small, and a long interval passes between two adjacent oscillations. Figure 7 (b)

shows the IR image at $t=1200$ s. Channels maintain their operation mode, and the operation of the working fluid of top channels is better than bottom channels during the operation. The working fluid in top channels is also used to drive bottom channels to improve the deterioration of heat transfer performance at the limit angle.

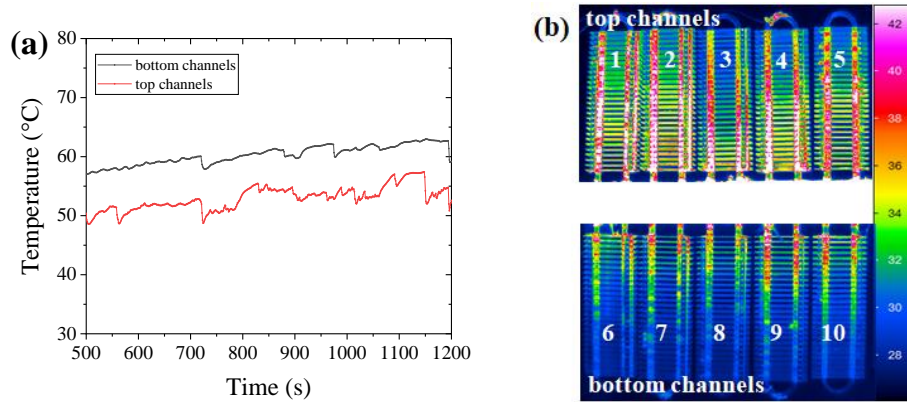


Fig. 7. The operation performance when the inclination angle is 0° ; (a) temperature profile; (b) IR temperature profiles for operation performance evaluation: the temperature scale is on the right.

Figure 8 (a) shows the temperature oscillation profile when the inclination angle is 90° . With the accumulation of heat, the temperature of the channel on the left side begins to show small irregular oscillations, while that on the right side shows periodic oscillations. The temperature of the left channel suddenly decreases, and the temperature is extremely close to that of the right channel after $t_A=883$ s. Figure 8 (b) shows the IR image at $t_B=1100$ s when the inclination angle is 90° . The temperature between adjacent channels on both sides is gradually decreasing from top to bottom. The flow mode of the working fluid is the same as that of single-row PHP with a lateral inclination of 90° [29]. This means that when the side inclination angle is 90° , the temperature oscillation mode of the double-row PHP on both sides is different at the time due to the random distribution of working fluid after start-up. However, with the accumulation of heat and the interaction of the working fluid flow, the working fluid will flow in the same way.

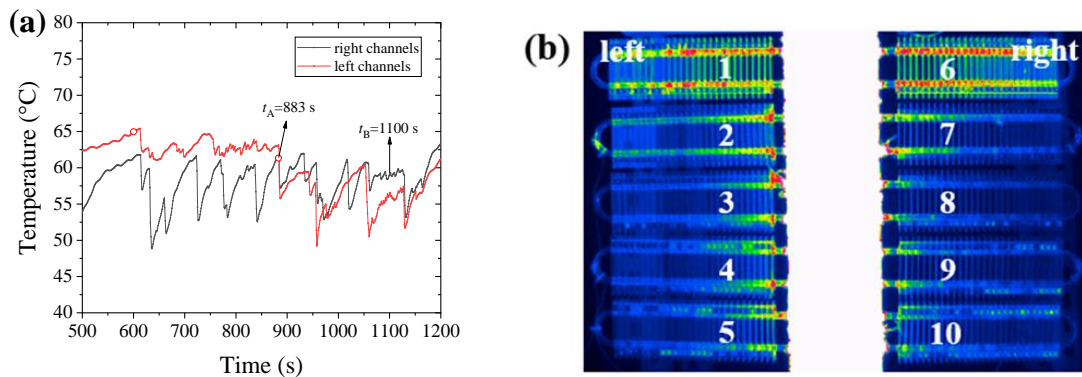


Fig. 8. The operation performance when the inclination angle is 90° ; (a) temperature profile; (b) IR temperature profiles for operation performance evaluation.

Figure 9 (a) shows the temperature oscillation profile when the inclination angle is 180° . Both sides have similar oscillation modes, showing intermittent oscillations. According to Figure 9 (b), the working fluid on both sides of the channels has a similar flow mode because the evaporation section is

located at the symmetry axis of the PHP, and the heat will also have a symmetrical diffusion trend during heating. Because the symmetry of the structure of double-row PHP and the heating position during the experiment is the symmetry axis, the pressure inside the tube tends to be symmetrical after start-up. The symmetrical structure and the heat source arrangement make the working fluid lack the flow force after the start-up, thus showing poor operation characteristics.

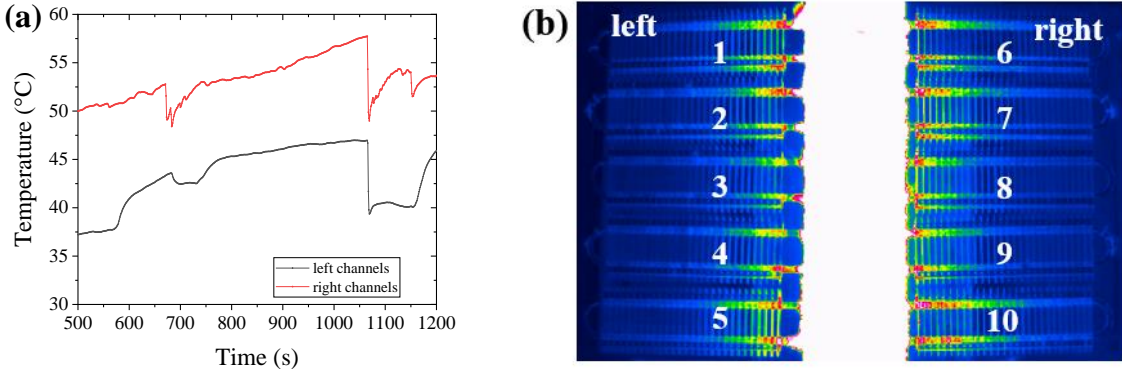


Fig. 9. The operation performance when the inclination angle is 180°; (a) temperature profile; (b) IR temperature profiles for operation performance evaluation.

3.3. Heat transfer performance at different inclination angles

Figure 10 shows the heat transfer resistance at different inclination angles. The thermal resistance increases within the range of 80~100 W and then begins to decrease when the inclination angle is 0° and 90°. The thermal resistance at the 180° angle is higher than in other angles. The thermal resistance is lower than other angles when the heat input amount is 140 W. When the inclination angle is 90°, the PHP needs higher heat input to achieve outstanding heat transfer performance, and the thermal resistance is the smallest compared with the other two cases.

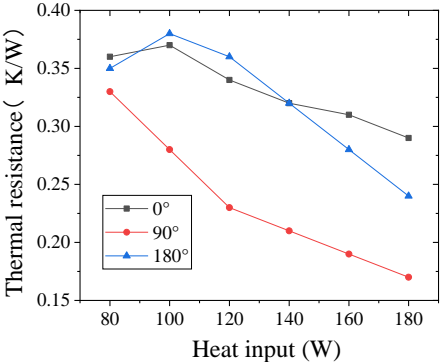


Fig. 10. Thermal resistance at inclination different angles

4. Conclusions

A single-layer double-row PHP is studied in this work. The structure of double-row PHP can effectively improve the problem of poor start-up performance of PHP with the limit angle. The mechanism of improving heat transfer performance was found through the analysis of temperature distribution by IR imager.

When the inclination angle is 0° , the problem that the PHP cannot start-up at the limit angle is improved by taking advantage of the structural characteristics of the double-row PHP. When the inclination angle is 90° , the start-up time is 209 s which is the shortest start time in this work. When the inclination angle is 180° , the start-up temperature is 43.2°C . This indicates that the PHP has the best temperature sensitivity.

When the inclination angle is 0° , top channels play active role in promoting the operation of bottom channels and improving the heat transfer performance. When the inclination angle is 90° , the flow mode of the working fluid gradually tends to be consistent under the action of the connecting pipe, and the working fluid is used to circulate in the tube. When the inclination angle is 180° , the symmetrical structure makes the working fluid flow difficult, and the heat transfer performance decreases.

The research in this work provides a idea for the structural design and optimization of the pulsating heat pipe.

Acknowledgment

This work was supported by the science and technology development project of Jilin province (Grant numbers 20190303113SF), and the industrial technology research and development project of Jilin province (2019C057-5).

Nomenclature

Q -effective heat input, [W] R -Thermal resistance, [$^\circ\text{C}/\text{W}$]
 T -temperature, [$^\circ\text{C}$] \bar{T} -average temperature, [$^\circ\text{C}$]
 d -critical diameter,[mm] e -uncertainty, [-]
 e_r -random uncertainty, [-] e_s -system uncertainty, [-]
 g -gravitational acceleration, [$\text{m}\cdot\text{s}^{-2}$] t -time, [s]
 ρ -density, [$\text{kg}\cdot\text{m}^{-3}$] δ -surface tension, [$\text{N}\cdot\text{m}^{-1}$]

References

- [1] C. Dang, *et al.*, Investigation on thermal design of a rack with the pulsating heat pipe for cooling CPUs, *Appl. Therm. Eng.*, 110 (2017), 5, pp 390-398. <https://doi.org/10.1016/j.applthermaleng.2016.08.187>
- [2] M. Uddin, *et al.*, Energy efficiency and low carbon enabler green IT framework for data centers considering green metrics, *Renew. Sust. Energy Rev.*, 16 (2012), 6, pp 4078-4094. <https://doi.org/10.1016/j.rser.2012.03.014>
- [3] A. Arya, *et al.*, Thermal performance analysis of a flat heat pipe working with carbon nanotube-water nanofluid for cooling of a high heat flux heater, *Heat Mass Transfer.*, 54 (2018), 4, pp 985-997. <https://doi.org/10.1007/s00231-017-2201-6>
- [4] M.M. Sarafraz, *et al.*, Assessment of the thermal performance of a thermosyphon heat pipe using zirconiaacetone nanofluids, *Renew. Energ.*, 136 (2019), ,pp 884-895. <https://doi.org/10.1016/j.renene.2019.01.035>

- [5] M.M. Sarafraz, *et al.*, Thermal evaluation of a heat pipe working with n-pentane-acetone and n-pentane-methanol binary mixtures, *J. Therm. Anal. Calorim.*, 139 (2020), 6, pp 2435-2445. <https://doi.org/10.1007/s10973-019-08414-2>
- [6] H. Akachi, Structure of a Heat Pipe, 1990, U.S. Patent 4921041.
- [7] S. Jun, *et al.*, Comparison of the thermal performances and flow characteristics between closed-loop and closed-end micro pulsating heat pipes, *Int. J. Heat Mass Tran.*, 95 (2016), 4, pp 890-901. <https://doi.org/10.1016/j.ijheatmasstransfer.2015.12.064>
- [8] S. Jun, *et al.*, Experimental investigation on the effect of the condenser length on the thermal performance of a micro pulsating heat pipe, *Appl. Therm. Eng.*, 130 (2018), 5, pp 439-448. <https://doi.org/10.1016/j.applthermaleng.2017.11.009>
- [9] V. Ayel, *et al.*, Experimental study of a closed loop flat plate pulsating heat pipe under a varying gravity force, *Int. J. Therm. Sci.*, 96 (2015), 10, pp 3–34. <https://doi.org/10.1016/j.ijthermalsci.2015.04.010>
- [10] S.M.Thompson, *et al.*, An experimental investigation of a three-dimensional flat-plate oscillating heat pipe with staggered microchannels. *Int. J. Heat Mass Tran.*, 54 (2011), 17, pp 3951-3959. <https://doi.org/10.1016/j.ijheatmasstransfer.2011.04.030>
- [11] Z. Xue, *et al.*, Experimental study on effect of inclination angles to ammonia pulsating heat pipe. *Chinese J. Aeronaut.*, 27 (2014), 5, pp 1122–1127. <https://doi.org/10.1016/j.cja.2014.08.004>
- [12] H. R. Goshayeshi, *et al.*, Experimental study on the effect of inclination angle on heat transfer enhancement of a ferrofluid in a closed loop oscillating heat pipe under magnetic field. *Exp. Therm. Fluid Sci.*, 74 (2016), 6, pp 265-270. <https://doi.org/10.1016/j.expthermflusci.2016.01.003>
- [13] Aboutalebi M, *et al.*, Experimental investigation on performance of a rotating closed loop pulsating heat pipe. *Int. Commun. Heat Mass*, 45 (2013), 7, pp 137-145. <https://doi.org/10.1016/j.icheatmasstransfer.2013.04.008>
- [14] Kelly B, *et al.*, Novel radial pulsating heat-pipe for high heat-flux thermal spreading. *Int. J. Heat Mass Tran.*, 121 (2018), 6, pp 97-106. <https://doi.org/10.1016/j.ijheatmasstransfer.2017.12.107>
- [15] Burbank G, *et al.*, Experimental investigation of a pulsating heat pipe for hybrid vehicle applications. *Appl. Therm. Eng.*, 50 (2013), 1, pp 94-103. <https://doi.org/10.1016/j.applthermaleng.2012.05.037>
- [16] P. Charoensawan, *et al.*, Closed loop pulsating heat pipes Part A: parametric experimental investigations. *Appl. Therm. Eng.*, 23 (2003), 16, pp 2009–2020. [https://doi.org/10.1016/S1359-4311\(03\)00159-5](https://doi.org/10.1016/S1359-4311(03)00159-5)
- [17] J. Lee, *et al.*, Effects of the number of turns and the inclination angle on the operating limit of micro-pulsating heat pipes. *Int. J. Heat Mass Tran.*, 124 (2018), 9, pp 1172–1180. <https://doi.org/10.1016/j.ijheatmasstransfer.2018.04.054>
- [18] K. H. Chien, *et al.*, A novel design of pulsating heat pipe with fewer turns applicable to all orientations. *Int. J. Heat Mass Tran.*, 55 (2012), 21, pp 5722-5728. <https://doi.org/10.1016/j.ijheatmasstransfer.2012.05.068>

- [19] M. Mameli, *et al.*, Thermal instability of a closed loop pulsating heat pipe: combined effect of orientation and filling ratio. *Exp. Therm. Fluid Sci.*, 59 (2014), 11, pp 222–229. <https://doi.org/10.1016/j.expthermflusci.2014.04.009>
- [20] N. Kammuang Lue, *et al.*, Correlation to predict the maximum heat flux of a vertical closed-loop pulsating heat pipe. *Heat Transfer Eng.*, 30 (2009), 12, pp 961–972. <https://doi.org/10.1080/01457630902837442>
- [21] T. Katpradit, *et al.*, Correlation to predict heat transfer characteristics of a closed end oscillating heat pipe at critical state. *Appl. Therm. Eng.*, 25 (2005), 14, pp 2138–2151. <https://doi.org/10.1016/j.applthermaleng.2005.01.009>
- [22] M. L. Rahman, *et al.*, An experimental investigation on the effect of fin in the performance of closed loop pulsating heat pipe (CLPHP). *Procedia Engineering*, 105 (2015), pp 137–144. <https://doi.org/10.1016/j.proeng.2015.05.049>
- [23] M. Li, *et al.*, Effect of filling ratio and orientation on the performance of a multiple turns helium pulsating heat pipe. *Cryogenics*, 100 (2019), 6, pp 62-68. <https://doi.org/10.1016/j.cryogenics.2019.04.006>
- [24] M. Ghanbarpour, *et al.*, Thermal performance of inclined screen mesh heat pipes using silver nanofluids. *Int. Commun Heat Mass*, 67 (2015), 10, pp 14-20. <https://doi.org/10.1016/j.icheatmasstransfer.2015.06.009>
- [25] J. Qu, *et al.*, Start-up, heat transfer and flow characteristics of silicon-based micro pulsating heat pipes. *Int. J. Heat Mass Tran.*, 55 (2012), 21, pp 6109-6120. <https://doi.org/10.1016/j.ijheatmasstransfer.2012.06.024>
- [26] V. K. Karthikeyan, *et al.*, Infrared thermography of a pulsating heat pipe: Flow regimes and multiple steady states. *Appl. Therm. Eng.*, 62 (2014), 2, pp 470-480. <https://doi.org/10.1016/j.applthermaleng.2013.09.041>
- [27] R. T. Dobson, *et al.*, Lumped parameter analysis of closed and open oscillatory heat pipes, in: *Proceedings of the 11th International Heat Pipe Conference*, Tokyo, Japan, 1999, pp 12–16.
- [28] S. J. Kline, *et al.*, Describing uncertainties in single-sample experiments, *Mech. Eng.* 75 (1953) pp 3-8.
- [29] F. M. Shang, *et al.*, An experimental investigation on heat transfer performance of pulsating heat pipe. *J. Mech. Sci. Technol.*, 34 (2020), 1, pp 425-433. <https://doi.org/10.1007/s12206-019-1241-x>

Submitted: 26.02.2021.

Revised: 23.06.2021.

Accepted: 24.06.2021.